JOURNAL OF CATALYSIS 114, 332–346 (1988)

Catalytic Anisotropy of MoO_3 in the Oxidative Ammonolysis of Toluene

ARNE ANDERSSON* AND STAFFAN HANSEN†

*Departments of *Chemical Technology and †Inorganic Chemistry 2, Chemical Center, Lund Institute of Technology, P.O. Box 124, S-221 00 Lund, Sweden*

Received June 15, 1987; revised March 17, 1988

The oxidative ammonolysis of toluene, i.e., ammoxidation without the presence of molecular oxygen, was studied over a series of samples of MoO_3 crystals. The specific surface areas of the various faces were determined from SEM micrographs. Correlations between activities and surface planes were found. For the formation of nitrile the specific activity decreased in the order {001} and {h01} > {100} > {010}. Also, for the formation of carbon oxides the terminations in the [001] direction were found to be especially active. These results are discussed in relation to surface structures and bond strength values of various oxygen species. It is concluded that the presence of both oxygen vacancies and nucleophilic oxygen species is a prerequisite for selective reaction to occur and that electrophilic oxygen species are the source for formation of carbon oxides. The characteristics of the various faces, as they emerge from the results on oxidative ammonolysis of toluene, seem to be of general significance for reactions occurring at the same types of active sites. They are shown to be applicable to results published in the literature on the oxidation of both propene and isobutene.

INTRODUCTION

The concepts of structure-insensitive (facile) reactions and structure-sensitive (demanding) reactions were introduced by Boudart (*1*). It was believed that in the rate-determining step of a facile reaction only one surface atom took part, and consequently little change of activity with structure could be expected in this case. On the other hand, in a demanding reaction several adjacent atoms were required, thus leading to a distinct change of activity with structure (*2*). Although the background for these concepts was found in results for hydrogen–hydrocarbon reactions over metals, the same concepts should in principle be valid also for oxidation reactions over metal oxides. However, no such results were reported until a few years ago (*3–16*). The reason might be that oxides are in some respects more complicated than metals. At the surfaces of metal oxides both metal ions and oxygen ions are exposed. The metal ions and oxygen ions can exist at several crystallographically nonequivalent positions, and even the valences of the cations can differ with respect to their position. At surfaces, oxygen species can exist in various forms, e.g., as O^-, O^{2-}, and –OH.

Concerning oxidation reactions over oxides, published results can be classified according to two types of structure sensitivity. The first type is where the turnover frequency of a specific species, on a specific face, depends on its environment. The second type is where activities and selectivities for various products are related to the distribution of crystal planes at the oxide surface. The first type of sensitivity has been extensively studied by Murakami and co-workers (*3–5*). They have studied various oxidation reactions over vanadium oxide catalysts and have calculated the turnover frequencies of V=O species. A sensitivity to structure, for example, was noted for the oxidation of CO, 1,3-butadiene, furan, and *n*-butane over unsupported vanadium oxide catalysts. Over the same catalysts the oxidation of H_2, ethane, ben-

0021-9517/88 $3.00

zene, and 1-butene were found to be structure-insensitive reactions. The authors suggested that, for the sensitive reactions, the active oxygen species are surface V=O groups located at, or close to, surface defects (*3*).

Several studies have been devoted to the second type of structure sensitivity. The oxidations of ethanol (*6*), methanol (*7*), and butenes (*8*) have been studied over unsupported MoO_3 crystals. Over graphite-supported MoO_3 crystals, the oxidations of propene (*9*), alcohols (*10*), and butenes (*11*) have been investigated. In addition to the results on MoO_3, investigations have been reported on the oxidation of *o*-oxylene (*12*) and methanol (*13, 14*) on V_2O_5, as have studies of the oxidation of propene and *o*-xylene on brannerite-type vanadates (*15, 16*). The term catalytic anisotropy has been introduced for the second type of structure sensitivity (*17*), which seems to reflect better its origin.

Concerning ammoxidation reactions, only a few results have been published showing the existence of catalytic anisotropy. It has been reported that the V_2O_5 (010) plane is selective for the formation of nicotinonitrile in the ammoxidation of 3-picoline (*18*). In the field of oxidative ammonolysis, i.e., ammoxidation carried out in the absence of gaseous oxygen, no results seem to have been published so far. In the present work, results are reported on the catalytic anisotropy of MoO_3 crystals in the oxidative ammonolysis of toluene. In the oxidation of propene over MoO_3, some controversy exists in ascribing the formation of products to specific planes (*9, 17, 19, 20*). Therefore, it was thought that the investigation of another reaction on MoO_3 could throw some new light on the role of the various MoO_3 planes in catalytic oxidation. The study of the oxidative ammonolysis of toluene is suitable for this purpose. The reason is that only lattice oxygen takes part in the formation of products. Furthermore, such a process has several advantages of industrial importance compared to that of ammoxidation (*21*). These are as follows: elimination of explosion hazards, elimination of nonselective radical oxidation in vapor phase, independent control of the product formation and the reoxidation of the reduced metal oxide, lower production costs due to reduction of the amount of noncondensables that must be handled, and a greatly reduced amount of waste gas from the product recovery sections.

METHODS

Preparation and characterization of catalysts. Samples of MoO_3 crystals were prepared by two methods. In the first method crystals were obtained by sublimation. The MoO_3 powder, Mallinckrodt analytical reagent, was heated just below its melting point (795°C) in a porcelain boat, which was placed in a stream of air. In the second method MoO_3 and B_2O_3 powders, BDH laboratory reagent, were heated for a few minutes in a porcelain crucible at approx. 700°C. The melt was then cooled and the solid obtained was washed with several portions of ethanol in order to remove all B_2O_3. The first method produced crystals of varying size, while the second method gave smaller crystals of more uniform dimensions, but of less regular appearance than in the first case. Additionally, the preparations were sieved into three fractions, S1–S3, using a set of sieves. Fraction S1 was obtained from the sample prepared by the use of a flux, while fractions S2 and S3 were obtained from sublimation.

Powder diffraction films taken with a Guinier–Hägg camera using Cu$K\alpha_1$ radiation showed sharp lines of a single phase, namely orthorhombic MoO_3. In order to characterize the crystal morphology, a series of scanning electron micrographs was taken of each sample with a JEOL T200 instrument. The thin flaky crystals were either sprinkled randomly onto the holder to allow for thickness measurements or arranged to lay flat on it, so that crystal length and width could be correctly measured. Each sample was covered with a thin layer

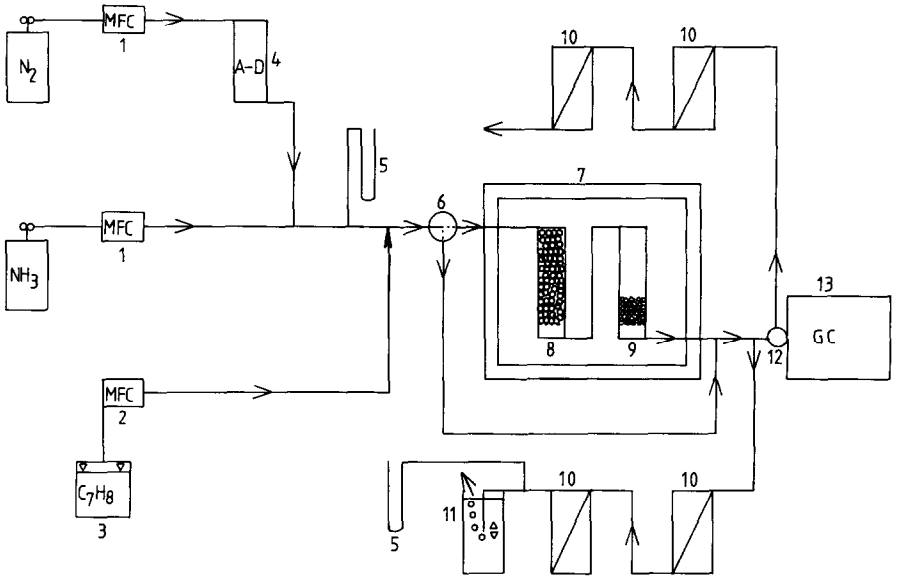

FIG. 1. Apparatus for investigation of oxidative ammonolysis of toluene. 1, Gas mass flow controllers; 2, liquid mass flow controller; 3, toluene supply; 4, Ascarite–Dehydrite; 5, manometers; 6, two-way valve; 7, oven; 8, preheater; 9, reactor; 10, condensers; 11, bleed-off tube; 12, gas sampling valve; and 13, gas chromatograph.

of gold before introduction into the scanning electron microscope (SEM).

Appartus. The apparatus used for the catalytic measurements is shown in Fig. 1. Nitrogen, which was fed as an inert carrier gas, and ammonia were supplied from pressure cylinders. Gas mass flow controllers (HI-TEC) were used to measure and control these flows. Toluene was supplied from a container, which was held under a pressure of nitrogen at 130 kPa. The flow was regulated by the use of a liquid mass flow controller (HI-TEC). Carbon dioxide was removed from the nitrogen stream by absorbing it in a tube filled with Ascarite and Dehydrite. Liquid toluene was introduced into the preheated mixture of nitrogen and ammonia, where it immediately evaporated. The reactant stream was then passed through a two-way valve. Depending upon the valve position, either the reactor could be by-passed for analysis of the inlet composition or the reactants could be transported through an oven (Pye). A preheater filled with glass rings, and a glass reactor with an internal diameter of 6 mm were positioned in the oven. The product stream was transported in heated glass tubes and then divided into two streams. One of the streams was passed through condensers and finally through a bleed-off tube, with which the outlet pressure from the reactor was controlled. The second stream was transported to a sampling valve, which was connected to a gas chromatograph.

Analysis. The products and unreacted toluene were analyzed with a Varian Vista 6000 gas chromatograph. The arrangement of columns and valve is shown in Fig. 2. A Valco six-port valve was used to inject a sample of 0.25 ml into the stream of carrier gas (N_2). The chromatographic system had three columns connected in series. The first column, 3 m × $\frac{1}{8}$ in., contained acid-washed Chromosorb W, 80–100 mesh, loaded with 20% SE-30. Via a Valco four-port valve this column could either be directly connected to the flame ionization detector (FID) or be connected to the other two columns. One of these, 1 m × $\frac{1}{8}$ in., was filled with Porapak

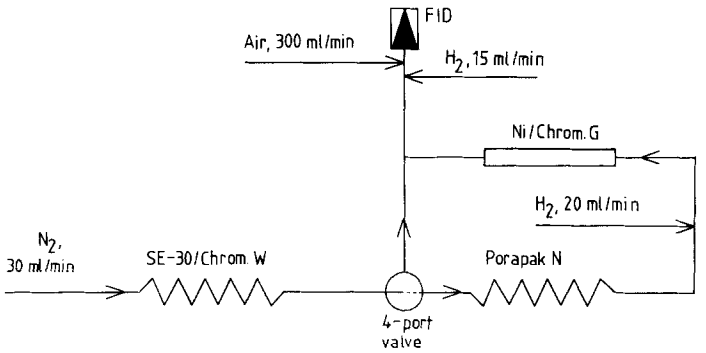

FIG. 2. Arrangement of chromatographic columns.

N, 80–100 mesh. The third column, 4 cm × $\frac{1}{8}$ in., was filled with 2% Ni on acid-washed Chromosorb G, 80–100 mesh. This column was kept in a separate oven, and always at 380°C. A stream of hydrogen was passed between the second and the third column.

When a sample was injected, the oven was kept at 80°C. At this temperature the carbon oxides rapidly passed through the first column and were separated on the second. On the third column, they were quantitatively converted to methane in the presence of hydrogen and could then be determined (*22–24*). Two minutes after injection, the four-port valve was switched. Then the carrier gas stream was directly connected to the detector, and the oven temperature increased linearly at 15°C/min from 80 to 150°C, where it was kept constant. Now the hydrocarbons were eluted and quantitatively determined. The chromatographic method used made it possible to analyze each injected sample for all components with high accuracy.

Experimental. The experiments were carried out slightly above atmospheric pressure in a differential reactor held at 452°C. An amount of 60–80 mg of MoO_3 crystals was used. The total inlet flow was 114 standard cm^3/min, and the concentrations were as follows: toluene 0.78 vol%, ammonia 2.63 vol%, and nitrogen 96.58 vol%. Conversions and yields were followed with time-on-stream. The first analysis was made after 1 min of reaction. Initial rates for nonreduced MoO_3 were obtained by extrapolation to initial time-on-stream, similar to the procedure described elsewhere (*18, 25, 26*). The MoO_3 crystals were heated up to reaction temperature in a flow of air to prevent prereduction.

RESULTS AND DISCUSSION

Morphological Characterization of MoO_3 Crystals

The morphology of the MoO_3 fractions can be illustrated by the two idealized crystals drawn in Fig. 3. The crystallographic setting is the same as that used by Kihlborg (*27*) in a crystal structure refinement. Thus the crystals are orthorhombic with $a = 3.96$ Å, $b = 13.9$ Å, and $c = 3.70$ Å, space group *Pbnm* and crystal class *mmm*. Only the three pinacoid faces are exposed on the left crystal, while the right is terminated by the dome {101}. Nordenskjöld, the polar ex-

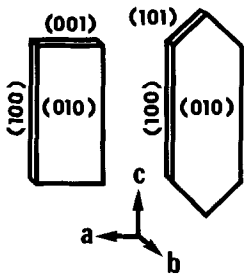

FIG. 3. Morphology of two idealized MoO_3 crystals of typical habit, i.e., flattened on {010}, and elongated along [001].

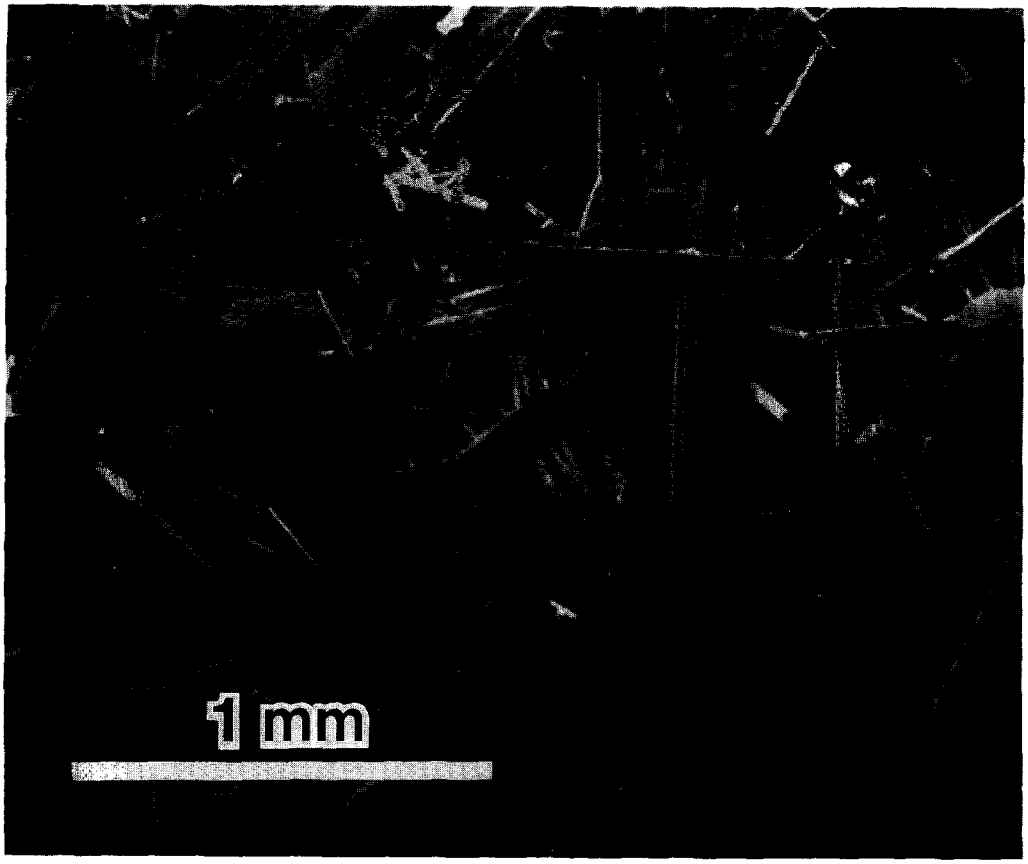

FIG. 4. SEM photograph of MoO_3 crystals in fraction S2.

plorer and mineralogist, described two additional domes, i.e., forms of the type {h01} (*28*). The habit of sublimed MoO_3 crystals is invariably described as flattened on {010} and elongated along [001]. For references, see Gmelin (*29*).

A typical crystal sample used in this study, S2, is pictured in Fig. 4. As can be seen the crystals are far from ideal in shape. The {010} and {100} faces are often well developed, while the terminations in the *c* direction consist of several different planes or are quite irregular. They are from now on designated "{001}" faces. Crystals exhibiting the fish tail habit observed by Nordenskjöld (*28*) were also found in the samples.

The dimensions of the MoO_3 crystals were measured with a ruler on SEM photographs. The thickness of the crystals, measured along [010], was found to be fairly constant for the three fractions compared to the variations in length and width. Since most crystals had a thickness in the range 4 to 10 μm, all crystals were assigned a thickness of 7 μm to be used in the calculations of specific face areas. Lengths and widths in the [001] and [100] directions, respectively, were, for each fraction, measured for 50 representative crystals. The data obtained are presented in Fig. 5.

In order to calculate the specific face areas of the crystals, they were treated as though they had a morphology and habit similar to those of the left crystal in Fig. 3. The product of thickness along [010] and width along [100] was used as a rough estimate of the area of the terminations in the

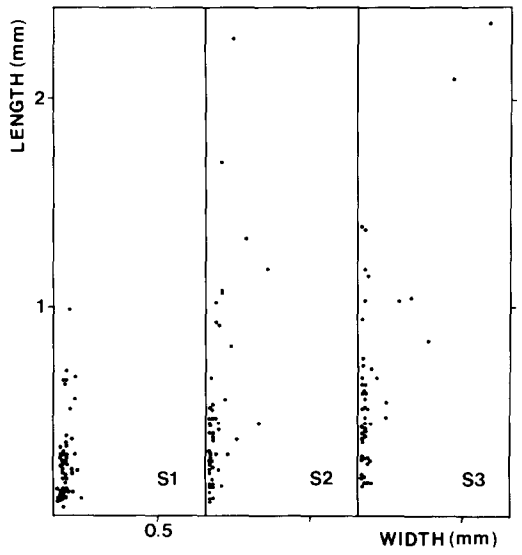

FIG. 5. Crystal dimensions as measured from SEM micrographs, including 50 crystals from each fraction.

[001] direction. Table 1 gives the resulting specific face areas. The area of each fraction was obtained by using the areas of 50 separate crystals, the crystal volume, and a density of 4.709 g/cm^3 (*30*).

Catalytic Activity and Activity–Plane Correlations

The initial reaction rates for the oxidative ammonolysis of toluene were measured over the three fractions. The data obtained are presented in Table 2. Only four products were formed. Benzonitrile was the major product, while carbon oxides were formed in small amounts. Also, traces of benzene could be detected over two fractions. From Table 2 it can be concluded that

TABLE 1

Specific Face Areas as Estimated from SEM Photographs

Sample	$A\{100\} \times 10^3$ (m^2/g)	$A\{010\} \times 10^2$ (m^2/g)	A"{001}" $\times 10^4$ [a] (m^2/g)	$\Sigma A \times 10^2$ (m^2/g)
S1	6.9	6.1	14.2	6.9
S2	5.5	6.1	5.6	6.7
S3	3.4	6.1	3.6	6.4

[a] Not well-defined planes on most crystals.

TABLE 2

Initial Reaction Rates for the Oxidative Ammonolysis of Toluene over MoO_3

Rates (mole/h, g)	Fractions		
	S1	S2	S3
CO, $\times 10^6$	1.59	1.40	1.33
CO_2, $\times 10^5$	2.36	1.47	1.25
C_6H_6, $\times 10^7$	2.4	1.3	0.0
C_6H_5CN, $\times 10^4$	3.13	2.03	1.43
Total, $\times 10^4$	3.38	2.17	1.57

the rates for the formation of products increase when they are compared from S3 to S1. With reference to Table 1, it appears that the specific surface area of the {010} faces is the same, while the specific surface areas of the {100} and "{001}" faces increase from S3 to S1. Thus, it can be concluded that {010} faces cannot be the only source for formation of any single product. However, it seems that {010} faces can considerably contribute to the formation of CO, since this rate is only weakly dependent upon the fraction used. On the other hand, this does not exclude the fact that the other faces which are less represented do have higher specific face activities.

Figure 6 shows the rates for the formation of CO_2 and nitrile as a function of the specific surface area of the {100} faces. It can be seen that in none of the cases is

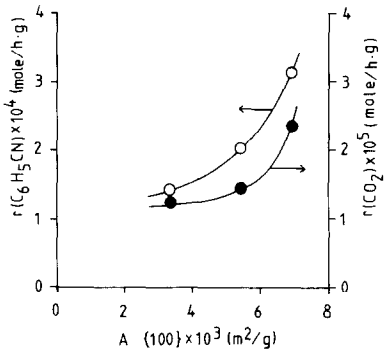

FIG. 6. Initial rates as a function of the specific surface area of {100} faces.

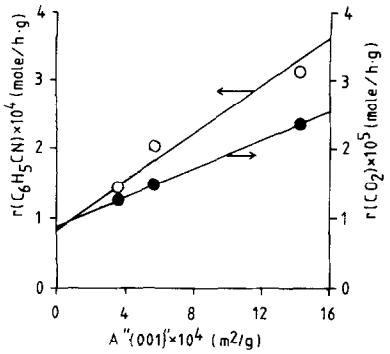

FIG. 7. Initial rates as a function of the specific surface area of "{001}" terminations.

there really a linear dependence. If the same data are plotted as a function of the specific surface area of the "{001}" terminations, Fig. 7, it is possible, for both products, to draw straight lines relatively close to the data points. However, in this case the lines do not pass through the origin. Considering these results, it can be concluded that the rates for formation of nitrile and CO_2 cannot be uniquely correlated to either {100} faces or "{001}" faces. Instead, the products are formed on more than one type of plane.

In order to determine definitively the specific face activities for the various products, a system of equations must be solved. In the system studied there are for each product three unknown specific face activities. For each crystal fraction, the specific surface area of each face has been determined, and the average rate for formation of each product has been measued. Considering the three fractions, the specific surface area of the {010} faces did not vary, while those of

TABLE 3

Specific Reaction Rates at MoO_3 Faces

Faces	$r(CO) \times 10^5$ (mole/h, m²)	$r(CO_2) \times 10^4$ (mole/h, m²)	$r(C_6H_5CN) \times 10^3$ (mole/h, m²)
{100}	1.4	0.2	19.1
{010}	2.0	1.4	0.7
"{001}"	19.9	104.0	96.2

TABLE 4

Selectivities at MoO_3 Faces

Faces	Sel. (CO) (%)	Sel. (CO_2) (%)	Sel. (C_6H_5CN) (%)
{100}	0.1	0.1	99.8
{010}	2.2	16.1	81.6
"{001}"	0.2	9.7	90.1

the {100} and "{001}" faces varied by factors approximately equal to 2 and 4, respectively. Therefore, it is possible to obtain rather accurate values when solving the system of equations comprising nine equations and nine unknown specific face activities. The result is presented in Table 3. It can be seen that all of the specific reaction rates calculated have positive values, which would not have been the case if the errors of the data were large.

Considering the results given in Table 3 it is possible to conclude as follows. The (100) face is active for the formation of benzonitrile, the (010) face has relatively low activities for the formation of both nitrile and carbon oxides, and the "(001)" terminations have high activities for the formation of all products. The selectivities for the various MoO_3 faces were calculated and are presented in Table 4. From this table it can be concluded that the (100) face is the most selective face for the formation of nitrile. If these conclusions are relevant then there must be some link between them and the surface structures of the various faces of MoO_3. This is considered in the next sections.

Structure of MoO_3

The structure of orthorhombic MoO_3 is schematically show in Fig. 8. Each molybdenum ion is surrounded by six closest neighboring oxygen ions, which are represented by idealized MoO_6 octahedra. However, these are in fact distorted since the molybdenum–oxygen distances vary between 1.67 and 2.33 Å (*27*). The structure

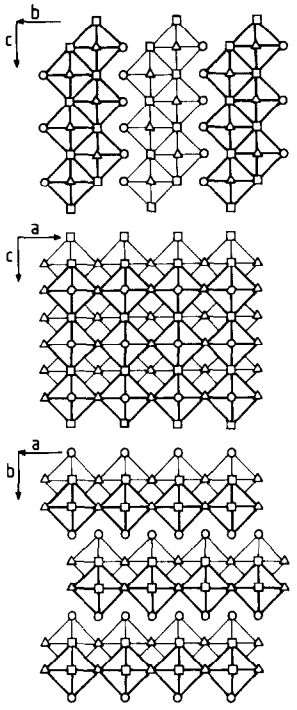

FIG. 8. Schematic presentation of the MoO_3 structure. The three crystallographically unequal oxygen ions O(1), O(2), and O(3) are denoted ○, △, and □, respectively.

can be described as a layer structure in which each layer is built up of MoO_6 octahedra at two levels, connected along [001] by common edges so as to form zigzag rows. Along [100] the octahedra have common corners only. The layers are held together by van der Waals forces. Three of the six oxygen ions surrounding every cation are thus common to three octahedra units, while two of them are shared between two units and one is unshared.

Relations between Activities and Bond Strength Values

Bond strength calculations combined with crystal structural considerations have been used to explain why the catalytic performances of crystallographically nonidentical planes can differ (*16, 17, 31–33*). It has been proposed that the bond strength values, *s*-values, are proportional to the bond energy of the metal–oxygen bond (*31, 33*). Evidence for this proposal exists (*34*). Therefore, as a generalization, oxygen positions characterized by a low sum of *s*-values can be expected to be vacant, at least at high temperatures. Moderate Σs-values can be anticipated to be characteristic for bonding between cations and electrophilic oxygen species. The reason is that the Σs-value in principle expresses the formal valence. It follows that bonding between cations and nucleophilic oxygen species should give relatively high Σs-values.

The *s*-values for the molybdenum–oxygen bonds in MoO_3 were calculated using the second approach Coulombic-type function derived by Ziółkowski (*35*). Table 5 gives the *s*-values for the individual bonds as well as the sum of the *s*-values for both

TABLE 5

Charge Distribution around Mo and O in MoO_3

Bond	d(Å)	$s(e^-)$ for Mo	$s(e^-)$ for		
			O(1)	O(2)	O(3)
Mo–O(1)	1.671	2.063	2.063		
Mo–O(2)	1.734	1.501		1.501	
Mo–O(2)	2.251	0.463		0.463	
Mo–O(3)	1.948	0.779			0.779
Mo–O(3)	1.948	0.779			0.779
Mo–O(3)	2.332	0.418			0.418
		$\Sigma = 6.003$	$\Sigma = 2.063$	$\Sigma = 1.964$	$\Sigma = 1.976$

TABLE 6

Surface Bond Strengths in MoO_3

Bond	Plane	d(Å)	$\Sigma s(e^-)$
Mo–O(2)	100	1.734	1.501
Mo–O(2)	100	2.251	0.463
Mo–O(1)	100	1.671	2.063
Mo–O(1)	010	1.671	2.063
Mo–O(3)	001	1.948	0.779
Mo–O(1)	001	1.671	2.063
Mo–O(3)	101	1.948	0.779
Mo–O(2)	101	1.734	1.501
Mo–O(2)	101	2.251	0.463
Mo–O(1)	101	1.671	2.063

molybdenum and the three crystallographically unequal oxygen species when they are fully coordinated. It is obvious that the formal valences obtained are very close to the theoretical values.

In the studies of the ammoxidation of 3-picoline (3-methylpyridine) over V_2O_5 catalysts some important relations between catalytic activity and bond strength values have been described (*18, 36*). It was found that nicotinonitrile was selectively formed at the (010) plane. This plane exposes both V^{5+} cations and nucleophilic oxygen species with $\Sigma s = 1.93$. The (100) and (001) planes were found to be the source for formation of carbon oxides. These planes were shown to accommodate single-coordinated electrophilic oxygen species having Σs-values equal to 0.48, 1.04, and 0.76. Table 6 presents the Σs-values of single coordinated oxygen species present at various surface planes of MoO_3. If the data in Tables 3 and 6 are compared with the results cited for the ammoxidation of 3-picoline over V_2O_5, then there are several common features that emerge. The (010) plane of MoO_3 was found to exhibit a very low activity for the formation of all products. According to the structure model, this plane is covered with double-bonded nucleophilic oxygen species having $\Sigma s = 2.06$. In comparison with the V_2O_5 (010) plane, it seems plausible that its low activity for the formation of nitrile is primarily due to the lack of exposed cations (oxygen vacancies). These are probably involved in a coordination of the aromatic ring to the surface, which seems to be a necessary step preceding the first hydrogen abstraction from the methyl group. Indeed, the mechanism for the selective ammoxidation of toluene over V_2O_5 has been found to include such a step (*37*). Further support for this conclusion is given by the fact that benzonitrile is selectively formed at the MoO_3 (100) plane, Table 4. The surface structure of this plane has some details in common with the V_2O_5 (010) plane. Both planes have zigzig chains of edge-sharing octahedra. A characteristic of two edge-sharing octahedra is that one of them projects a double-bonded oxygen species, while the other exposes a naked cation. The oxygen positions at MoO_3 (100) with $\Sigma s = 0.46$ are probably vacant at a reaction temperature of 452°C. Such an assumption is in agreement with results obtained over V_2O_5, indicating that oxygen positions having $\Sigma s = 0.48$ are largely vacant at 250° (*36*). Both the (010) and the (100) faces of MoO_3 have low activities for the formation of carbon oxides. Table 6 shows that there are no oxygen positions at these planes that have Σs-values in the range characteristic for electrophilic oxygen species. Such characteristic values should be neither too low nor too high. The ammoxidation results for V_2O_5 indicate that Σs-values in this case should be around 0.7–1.1, which also is supported by results showing that V_2O_5 (100) and (001) planes are nonselective in the oxidation of *o*-xylene (*12*).

The terminations in the [001] direction of the MoO_3 samples used were found to consist of {001} and {h01} faces. Table 6 includes Σs-values for single coordinated oxygen positions at the (001) and (101) faces. The latter can be considered representative for all types of {h01} faces since in fact these can be treated as combinations of (100) and (001) faces. The table shows that both the (001) and the (101) planes expose

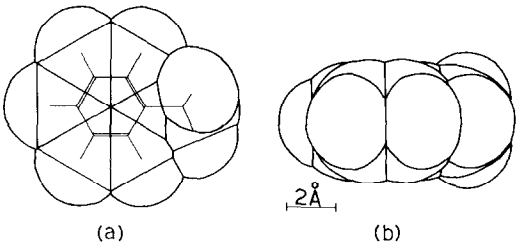

FIG. 9. Van der Waals model of toluene. (a) Top view, and (b) side view.

nucleophilic double-bonded oxygen species with Σs-values equal to 1.50 and 2.06 as well as electrophilic species characterized by $\Sigma s = 0.78$. Positions with $\Sigma s = 0.46$ can be treated as vacancies, as mentioned above. Data given in Table 3 show that both carbon oxides and nitrile are formed at the so-called "{001}" terminations. The reason that carbon oxides are produced at these terminal planes is that as with the (100) and (001) planes of V_2O_5 they expose electrophilic oxygen species. Activity data of the present investigation concern ammoxidation carried out in the absence of molecular oxygen. A consequence of this is that when carbon oxides are formed, a relatively high concentration of oxygen vacancies is created at the surface due to slow diffusion of oxygen from the bulk. These vacancies together with the nucleophilic oxygen species form the prerequisite for selective reaction to occur, and thus nitrile can be formed. Consequently, the relation between bond strength values and activities for selective and nonselective reaction on various planes of V_2O_5 and MoO_3 has been clearly established.

Adsorption of Toluene at Various Planes

In order to determine if there are any structural limitations for selective or nonselective reactions to occur at specific planes, a model of a toluene molecule has been placed in contact with various surfaces of MoO_3. Surface structures obtained from extension of the idealized bulk structure are used as a first approximation to roughly evaluate the probability for reaction to occur. For the ionic radius of oxygen a value of 1.40 Å is used (*38*). An overlap between the ionic radius of oxygen and the van der Waals radius of carbon or methyl hydrogen is used as a criterion for reaction to take place. This is not unreasonable since at elevated temperatures bond distances are elongated compared to those determined at room temperature. The van der Waals radii for hydrogen and carbon are 1.500 and 1.900 Å, respectively (*39, 40*). Figure 9 shows a van der Waals model of a toluene molecule with a more common representation being inserted for comparison. The latter representation is used for clarity in the illustrations of the adsorption of toluene at various planes, Figs. 10–12. However, it should be remembered that the molecule is actually much more bulky, and both the molecule and the atoms are vibrating. In the case of nonselective reaction, the methyl group is not shown in the figures since its position is not of primary interest. No mechanistic details are elaborated in the treatment, and the possibilities of selective and nonselective reaction are concluded from a few simple criteria. These are as follows. Nonselective reaction is possible on the condition that there can be an interaction between electrophilic oxygen species and the ring of toluene. Such oxygen species attack the molecule in the region of its highest electron density, which leads to degradation. The degradation products can then react to form carbon oxides (*41*). Selective reaction is considered possible when simultaneously both a coordination of

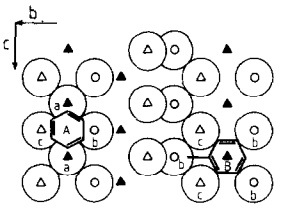

FIG. 10. Single coordinated oxygen species at the idealized (100) plane of MoO_3. O(a), $\Sigma s = 0.46$; O(b), $\Sigma s = 2.06$; O(c), $\Sigma s = 1.50$; and ▲, Mo.

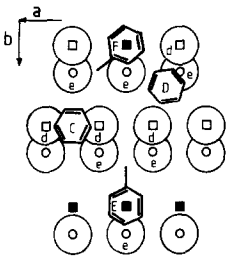

FIG. 11. Single coordinated oxygen species at the idealized (001) plane of MoO_3. O(d), $\Sigma s = 0.78$; O(e), $\Sigma s = 2.06$; and ■, Mo.

the aromatic ring to a cation and an interaction between the methyl group and some nucleophilic oxygen species occur. Since the stoichiometric reaction to nitrile requires three oxygen species, positions which enable the methyl group to be surrounded by preferably not less than three positions of nucleophilic oxygen are sought. One of the nucloephilic oxygen species can react with ammonia to give water and a =NH species, which can then react with the methyl carbon atom to give nitrile (*42*).

Figure 10 shows two cases of different types of reaction at the (100) plane. Case A shows that when electrophilic O(a) species with $\Sigma s = 0.46$ are present at the surface, it is possible for them to attack the electron-rich toluene ring, which after additional steps results in the formation of carbon oxides. However, since the concentration of O(a) species is low, total combustion does not occur to a large extent. Case B shows that it is possible to coordinate the ring at a molybdenum ion situated in a surrounding of five nucleophilic oxygen species, O(b) and O(c) with Σs equal to 2.06 and 1.50, respectively. Three of these oxygen species are localized in the immediate vicinity of the methyl group, thus permitting a reaction to nitrile without rotation of the toluene molecule.

Figure 11 illustrates four possible situations at the (001) plane. Cases C and D show that it is possible to have an electrophilic attack simultaneously with two O(d) species having $\Sigma s = 0.78$. After formation of carbon oxides, naked molybdenum ions are exposed. This is especially the case in oxidative ammonolysis. The ring of toluene can be coordinated at these molybdenum ions. In cases E and F the adsorbed molecule is surrounded by three nucleophilic O(e) species with $\Sigma s = 2.06$. All of them can interact with the methyl group on the condition that the toluene molecule is allowed to rotate.

In Fig. 12 some possibilities for absorption of toluene at the (101) plane are drawn schematically. Cases G and H illustrate the possibilities for electrophilic oxygen species with $\Sigma s = 0.78$ to take part in a degradation of the aromatic ring. In case G, a coordination of the ring to a cation and an attack by electrophilic species can occur simultaneously. Cases I, J, and K show that the methyl group will be surrounded by several nucleophilic oxygen species after toluene is adsorbed at a cation. In cases I and J the methyl group can reach three positions for O(g) species having $\Sigma s = 2.06$. The adsorption in case K results in a configuration where the methyl group is rather close to two O(g) species and two O(h) species.

From Figs. 9–12 it thus can be concluded that the conclusions drawn about selective and nonselective reactions based on bond strength values still hold even when geometric factors are taken into consideration.

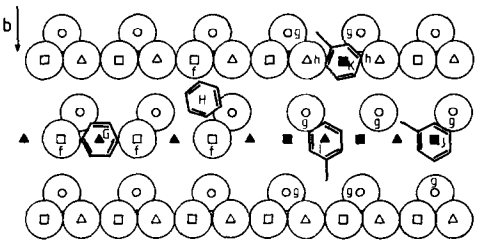

FIG. 12. Single coordinated oxygen species at the idealized (101) plane of MoO_3. O(f), $\Sigma s = 0.78$; O(g), $\Sigma s = 2.06$; O(h), $\Sigma s = 1.50$; ■ and ▲ are Mo exposed at vacant oxygen positions having Σs-values of 0.78 and 0.46, respectively.

TABLE 7

Face Specificity of MoO_3 in Oxidation of Propene

Reference	Planes			
	(100)	(010)	(101)	(001)
(9)	A[a]	C[a]		
(19)	A	C	A	A
(17)	C		A	A
(20)	A, C	C	A, C	A, C
This work	A		A, C	A, C

[a] A, acrolein; C, CO_2.

Oxidation of Propene and Isobutene

In a study of the oxidation of propene over graphite-supported MoO_3 catalysts Volta *et al.* (*9*) concluded that acrolein was formed at the (100) plane and CO_2 at the (010) plane. Later, Volta and Tatibouet (*19*) presented an improvement in the interpretation of these results. It was then concluded that acrolein was formed at (100), (101), and (001) planes, while CO_2 was exclusively formed at the (010) plane. However, Ziółkowski (*17*) has shown that it is possible to correlate the same data in alternative ways. On the basis of a crystallochemical model of active sites, this author concluded that acrolein was formed at (101) and (001) planes, CO_2 at (100) planes, and the (010) plane was inactive. Recently, Brückman *et al.* (*20*) have shown that it is also possible to explain the same experimental data on the assumption that CO_2 was formed at all planes and that the rate-determining step in the formation of acrolein occurred at (100), (101), and (001) planes. In this case, it was argued that the (010) plane was responsible for the insertion of oxygen, i.e., a two-plane mechanism. The various interpretations are summarized in Table 7, which also includes what should be expected on the basis of our results on oxidative ammonolysis of toluene. The conclusions drawn in the present investigation about the nature of various MoO_3 planes, if relevant, should be of a more general significance. The formation of acrolein from propene requires an active site that can attract the electrons of the double bond, abstract two hydrogen atoms, and insert a nucleophilic oxygen species (*41–43*). It has been demonstrated above that such sites exist at (100), (101), and (001) planes. Furthermore, electrophilic oxygen species taking part in combustion of toluene can attack the double bond of propene as well, resulting in degradation. Thus, it can be expected that also in the oxidation of propene, CO_2 should be formed mainly at (101) and (001) planes.

The oxidation of isobutene over graphite-supported MoO_3 has also been investigated by Volta *et al.* (*11*). They concluded that methacrolein was formed at the (100) and (101) faces. In this case, the formation of CO_2 was found to be related to the (100) plane, while the (010) plane was concluded to be inactive. In our opinion, it seems somehow contradictory to conclude that CO_2 is formed at planes completely different from propene and isobutene, respectively. In both cases, combustion should involve reaction with electrophilic oxygen species, while selective reaction should include insertion of nucleophilic oxygen (*41, 43*). Therefore an attempt was made to correlate the experimental data of Volta and co-workers, obtained for oxidation of propene and isobutene, respectively, to the general face activity pattern that has emerged in the present work, which

TABLE 8

Relative Reaction Rates at MoO_3 Faces in the Oxidations of Propene and Isobutene

Reference	Product	Relative rates			
		(100)	(010)	(101)	(001)
(19)	Acrolein	2.264	0.063	0.700	0.700
	CO_2	0	1.000	0	0
This work	Acrolein	0.138	0	1.438	2.157
	CO_2	0	0.201	1.000	1.000
(11)	Methacrolein	0.55	0	0.13	0.13
	CO_2	1.00	0	0	0
This work	Methacrolein	0	0	0.688	0.688
	CO_2	0	0	1.000	1.000

TABLE 9

Ratios of Selectivities for Formation of Acrolein (S_A) and Methacrolein (S_{MA}) to the Selectivity for Formation of CO_2 (S_C)

Sample[a]	S_A/S_C			S_{MA}/S_C		
	Exp.	(*19*)	This work	Exp.	(*11*)	This work
420-6	0.39	0.37	0.39	0.67	0.62	0.69
420-61	0.59	0.61	0.59	0.65	0.62	0.69
471-6	0.95	0.97	0.98	0.78	0.70	0.69
496-6	0.94	0.90	0.92	0.67	0.68	0.69
496-61	1.44	1.43	1.44	0.69	0.63	0.69

[a] Notations from Refs. (*9, 19*).

should be possible due to the mechanistic similarities. The results obtained are included in Tables 8 and 9. It can be seen that the correlations obtained, if compared with those presented by Volta *et al.* (*11, 19*), fit better with experimental data.

CONCLUSIONS

In the present investigation of the oxidative ammonolysis of toluene over MoO_3, it has been found that selective reaction to benzonitrile occurs at {100}, {001}, and {h01} faces, while total combustion takes place at {001} and {h01} faces.

It has been demonstrated, using bond strength calculations combined with crystallographic considerations, that sites active for formation of nitrile consist of a cation surrounded by nucleophilic oxygen species in a suitable geometrical configuration. The cation is an adsorption site for the toluene ring and the nucleophilic oxygen species take part in the abstraction of hydrogen atoms form the methyl group. Furthermore, one of the nucleophilic species reacts with ammonia to give an imido species which then acts as a N-insertion center. A prerequisite for nonselective reaction to occur is the existence of unsaturated electrophilic oxygen species, which attack the electron-rich part of the reacting molecule, finally resulting in formation of carbon oxides.

Additional support for the conclusions presented about the nature of various MoO_3 faces is given considering data published on other reactions, involving the same type of sites for selective and nonselective reaction, respectively. It is shown that the results obtained by Volta and co-workers for oxidations of propene (*9, 19*) and isobutene (*11*) over well-defined graphite-supported MoO_3 crystals can be correlated to the general face activity pattern that is observed to be valid for the oxidative ammonolysis of toluene. The correlation, which excellently fits experimental data, is different from those presented by others (*9, 19, 17, 20*).

Brückman *et al.* (*20*) have found a correlation between the (010) plane and the formation of acrolein from allyl species generated by decomposition of allyl iodide and bromide. This result is not contradictory to our results, since the (010) plane accommodates nucleophilic oxygen species, cf. Table 6, which can react with radicals generated somewhere else. However, these authors suggested that also in the oxidation of propene the oxygen insertion occurs at {010} faces, while the initial hydrogen abstraction occurs at perpendicular faces. They showed that the results of Volta *et al.* (*9*) can be correlated to such a model. Unfortunately, due to their assumption that the oxygen insertion is a fast step, the implication is that the same correlation is still valid irrespectively of the faces at which the oxygen insertion occurs. According to our model, a two-plane mechanism is not likely or necessary since {100}, {101}, and {001} faces also accommodate nucleophilic oxygen species.

In the present investigation, absolute values of specific reaction rates at various MoO_3 faces have been calculated. Absolute activity values are desirable in order to make possible a comparison between different oxides, which is necessary for an industrial choice of catalyst type. Such correlations have not previously been given for reactions over unsupported MoO_3 crystals

(*6–8*). Instead, selectivity data have been used to find correlations. This method permits the calculation of relative activities, a procedure which suffers from the fact that some of the face activity values are set equal to one. If the real values of these parameters happen to be equal to zero, then faulty correlations are obtained. This fact does not seem to have been considered in investigations where this method has been used (*8, 10, 11, 19*). In the case when MoO_3 is supported on graphite (*9–11*), no absolute face activity values can be calculated due to difficulties in the determination of the surface fraction that is covered with MoO_3.

ACKNOWLEDGMENT

The authors gratefully acknowledge financial support from the National Swedish Board for Technical Development (STU).

REFERENCES

1. Boudart, M., *in* "Advances in Catalysis" (D. D. Eley, H. Pines, and P. B. Weisz, Eds.), Vol. 20, p. 153. Academic Press, New York, 1969.
2. Boudart, M., *in* "Proceedings, 6th International Congress on Catalysis, London, 1976," Vol. 1, p. 1. The Chemical Society, London, 1977.
3. Mori, K., Miyamoto, A., and Murakami, Y., *Appl. Catal.* **6,** 209 (1983).
4. Mori, K., Miyamoto, A., and Murakami, Y., *J. Phys. Chem.* **88,** 2741 (1984).
5. Miyamoto, A., Mori, K., Miura, M., and Murakami, Y., *in* "Studies in Surface Science and Catalysis" (M. Che and G. C. Bond, Eds.), Vol. 21, p. 371. Elsevier, Amsterdam, 1985.
6. Tatibouet, J. M., and Germain, J. E., *J. Chem. Res. (M),* 3070 (1981).
7. Tatibouet, J. M., and Germain, J. E., *J. Catal.* **72,** 375 (1981).
8. Tatibouet, J. M., Phichitkul, Ch., and Germain, J. E., *J. Catal.* **99,** 231 (1986).
9. Volta, J. C., Forissier, M., Theobald, F., and Pham, T. P., *Faraday Discuss. Chem. Soc.* **72,** 225 (1981).
10. Tatibouet, J. M., Germain, J. E., and Volta, J. C., *J. Catal.* **82,** 240 (1983).
11. Volta, J. C., Tatibouet, J. M., Phichitkul, Ch., and Germain, J. E., *in* "Proceedings, 8th International Congress on Catalysis, Berlin 1984," Vol. IV, p. 451. Verlag Chemie, Weinheim, 1984.
12. Gasior, M., and Machej, T., *J. Catal.* **83,** 472 (1983).
13. Tatibouet, J. M., and Germain, J. E., *C. R. Acad. Sci. Paris* **296**(2), 613 (1983).
14. Baiker, A., and Monti, D., *J. Catal.* **91,** 361 (1985).
15. Ziółkowski, J., and Janusz, J., *J. Catal.* **81,** 298 (1983).
16. Ziółkowski, J., and Gasior, M., *J. Catal.* **84,** 74 (1983).
17. Ziółkowski, J., *J. Catal.* **80,** 263 (1983).
18. Andersson, A., Bovin, J.-O., and Walter, P., *J. Catal.* **98,** 204 (1986).
19. Volta, J. C., and Tatibouet, J. M., *J. Catal.* **93,** 467 (1985).
20. Brückman, K., Grabowski, R., Haber, J., Mazurkiewicz, J., Słoczynski, J., and Wiltowski, T., *J. Catal.* **104,** 71 (1987).
21. Sze, M. C., and Gelbein, A. P., *Hydrocarbon Process.* **55**(2), 103 (1976).
22. Porter, K., and Volman, D. H., *Anal. Chem.* **34,** 748 (1962).
23. Williams, F. W., Woods, F. J., and Umstead, M. E., *J. Chromatogr. Sci.* **10,** 570 (1972).
24. Tesarik, K., and Krejci, M., *J. Chromatogr.* **91,** 539 (1974).
25. Andersson, A., and Lundin, S. T., *J. Catal.* **58,** 383 (1979).
26. Andersson, A., and Lundin, S. T., *J. Catal.* **65,** 9 (1980).
27. Kihlborg, L., *Ark. Kem.* **21,** 357 (1963).
28. Nordenskjöld, A. E., *Poggendorffs Ann. Phys. Chem.* **112,** 160 (1861).
29. "Gmelins Handbuch der Anorganischen Chemie," Molybdän, Ergänzungsband, Teil B1, p. 86. Springer-Verlag, Berlin, 1975.
30. Swanson, H. E., Fuyat, R. K., and Ugrinic, G. M., "Natl. Bur. Stand. Circ.," No. 539, Vol. 3, p. 30. 1954.
31. Andersson, A., *J. Solid State Chem.* **42,** 263 (1982).
32. Ziółkowski, J., *J. Catal.* **81,** 311 (1983).
33. Ziółkowski, J., *J. Catal.* **84,** 317 (1983).
34. Ziółkowski, J., and Dziembaj, L., *J. Solid State Chem.* **57,** 291 (1985).
35. Ziółkowski, J., *J. Solid State Chem.* **57,** 269 (1985).
36. Andersson, A., *J. Catal.* **100,** 414 (1986).
37. Andersson, A., and Otamiri, J. C., *in* "Preprints, Symp. on Hydrocarbon Oxidation, New Orleans, 1987." American Chemical Society, Washington, DC, 1987.
38. Pauling, L., "The Nature of the Chemical Bond." Cornell Univ. Press, New York, 1963.
39. Allinger, N. L., *in* "Advances in Physical Organic Chemistry" (V. Gold and D. Bethell, Eds.), Vol. 13, p. 1. Academic Press, New York, 1976.
40. Burkert, U., and Allinger, N. L., "Molecular Mechanics," ACS Monograph 177. American Chemical Society, Washington, DC, 1982.

41. Haber, J., *in* "Solid State Chemistry in Catalysis" (R. K. Grasselli and J. F. Brazdil, Eds.), ACS Symposium Series, Vol. 279, p. 1. American Chemical Society, Washington, DC, 1985.
42. Grasselli, R. K., Brazdil, J. F., and Burrington, J. D., *in* "Proceedings, 8th International Congress on Catalysis, Berlin, 1984," Vol. 5, p. 369. Verlag Chemie, Weiheim, 1984.
43. Haber, J., *in* "Surface Properties and Catalysis by Non-metals" (J. P. Bonnelle, B. Delmon, and E. Derouane, Eds.), NATO ASI Series, Ser. C, No. 105, p. 1. Reidel, Dordrecht, 1983.